nature medicine

ABT-199, a potent and selective BCL-2 inhibitor, achieves antitumor activity while sparing platelets

Andrew J Souers[1], Joel D Leverson[1], Erwin R Boghaert[1], Scott L Ackler[1], Nathaniel D Catron[1], Jun Chen[1], Brian D Dayton[1], Hong Ding[1], Sari H Enschede[1], Wayne J Fairbrother[2], David C S Huang[3,4], Sarah G Hymowitz[2], Sha Jin[1], Seong Lin Khaw[3,4], Peter J Kovar[1], Lloyd T Lam[1], Jackie Lee[2], Heather L Maecker[2], Kennan C Marsh[1], Kylie D Mason[3–5], Michael J Mitten[1], Paul M Nimmer[1], Anatol Oleksijew[1], Chang H Park[1], Cheol-Min Park[1,7], Darren C Phillips[1], Andrew W Roberts[3–5], Deepak Sampath[2], John F Seymour[4,6], Morey L Smith[1], Gerard M Sullivan[1], Stephen K Tahir[1], Chris Tse[1], Michael D Wendt[1], Yu Xiao[1], John C Xue[1], Haichao Zhang[1], Rod A Humerickhouse[1], Saul H Rosenberg[1] & Steven W Elmore[1]

Proteins in the B cell CLL/lymphoma 2 (BCL-2) family are key regulators of the apoptotic process. This family comprises proapoptotic and prosurvival proteins, and shifting the balance toward the latter is an established mechanism whereby cancer cells evade apoptosis. The therapeutic potential of directly inhibiting prosurvival proteins was unveiled with the development of navitoclax, a selective inhibitor of both BCL-2 and BCL-2–like 1 (BCL-X_L), which has shown clinical efficacy in some BCL-2–dependent hematological cancers. However, concomitant on-target thrombocytopenia caused by BCL-X_L inhibition limits the efficacy achievable with this agent. Here we report the re-engineering of navitoclax to create a highly potent, orally bioavailable and BCL-2–selective inhibitor, ABT-199. This compound inhibits the growth of BCL-2–dependent tumors *in vivo* and spares human platelets. A single dose of ABT-199 in three patients with refractory chronic lymphocytic leukemia resulted in tumor lysis within 24 h. These data indicate that selective pharmacological inhibition of BCL-2 shows promise for the treatment of BCL-2–dependent hematological cancers.

Apoptosis, or programmed cell death, is a conserved and regulated process that is the primary mechanism for the removal of aged, damaged and unnecessary cells. The ability to block apoptotic signaling is a key hallmark of cancer and is thus important for oncogenesis, tumor maintenance and chemoresistance[1]. Dynamic binding interactions between prodeath (for example, BCL-2–associated X protein (BAX), BCL-2 antagonist/killer 1 (BAK), BCL-2–associated agonist of cell death (BAD), BCL-2–like 11 (BIM), NOXA and BCL-2 binding component 3 (PUMA)) and prosurvival (BCL-2, BCL-X_L, BCL-2–like 2 (BCL-W), myeloid cell leukemia sequence 1 (MCL-1) and BCL-2–related protein A1 (BFL-1)) proteins in the BCL-2 family control commitment to programmed cell death. Altering the balance among these opposing factions provides one means by which cancer cells undermine normal apoptosis and gain a survival advantage[2,3].

BCL-2, the first identified apoptotic regulator, was originally cloned from the breakpoint of a t(14;18) translocation present in human B cell lymphomas[2,4–6]. This protein has since been shown to have a dominant role in the survival of multiple lymphoid malignancies[7,8]. BCL-X_L was subsequently identified as a related prosurvival protein and is associated with drug resistance and disease progression of multiple solid-tumor and hematological malignancies[5,9,10]. We have previously established that BCL-X_L is also the primary survival factor in platelets[11,12]. Genetic ablation, hypomorphic mutation or pharmacologic inhibition of BCL-X_L results in reduced platelet half-life and dose-dependent thrombocytopenia *in vivo*[12].

The association of prosurvival BCL-2 family members with tumor initiation, disease progression and drug resistance makes them compelling targets for antitumor therapy[2]. Despite the fact that direct antagonism of proteins in the BCL-2 family requires disruption of protein-protein interactions, the use of structure-based drug design has recently rendered these proteins tractable targets[13]. We previously reported navitoclax (ABT-263), an orally bioavailable small molecule with a high affinity for both BCL-2 and BCL-X_L that is currently being evaluated in phase 2 clinical trials[14–18]. Both the antitumor efficacy and hematologic toxicities of navitoclax are dictated by its inhibition profile of prosurvival proteins in the BCL-2 family. Early signs of clinical antitumor activity have been observed in lymphoid malignancies thought to be dependent on BCL-2 for survival[16,17]. As predicted by preclinical data, inhibition of BCL-X_L by navitoclax induces a rapid, concentration-dependent decrease in the number

[1]AbbVie Inc., North Chicago, Illinois, USA. [2]Genentech, Inc., South San Francisco, California, USA. [3]The Walter and Eliza Hall Institute of Medical Research, Parkville, Victoria, Australia. [4]Faculty of Medicine, Dentistry and Health Sciences, University of Melbourne, Melbourne, Victoria, Australia. [5]Department of Clinical Hematology and Bone Marrow Transplantation, Royal Melbourne Hospital, Parkville, Victoria, Australia. [6]Department of Hematology, Peter MacCallum Cancer Centre, Melbourne, Victoria, Australia. [7]Present address: Division of Chemistry and Biological Chemistry, School of Physical and Mathematical Sciences, Nanyang Technological University, Singapore. Correspondence should be addressed to A.J.S. (andrew.souers@abbvie.com).

Received 17 July 2012; accepted 29 November 2012; published online 6 January 2013; doi:10.1038/nm.3048

of circulating platelets. This mechanism-based thrombocytopenia is the dose-limiting toxicity of single-agent navitoclax treatment in patients and limits the ability to drive drug concentrations into a highly efficacious range. We hypothesized that a BCL-2–selective (BCL-X_L–sparing) inhibitor would culminate in substantially reduced thrombocytopenia while maintaining efficacy in lymphoid malignancies. The resulting increase in the therapeutic window should allow for greater BCL-2 suppression and clinical efficacy in BCL-2–dependent tumor types.

The generation of BCL-2–selective inhibitors is complicated by the high degree of similarity within the BH3-binding domains of BCL-2 and BCL-X_L[19]. To circumvent this challenge, we exploited a unique BCL-2–small molecule cocrystal structure to guide the rational design of ABT-199, a first-in-class BCL-2–selective inhibitor that causes substantially less platelet killing *ex vivo* and *in vivo* as compared to navitoclax. In addition to showing preclinical efficacy in BCL-2–dependent cell lines and tumor xenograft models, ABT-199 demonstrated immediate antileukemic activity after a single dose in three patients with refractory chronic lymphocytic leukemia (CLL) while causing only minor changes in platelet counts. These data support the hypothesis that potent and selective BCL-2 inhibitors such as ABT-199 have the potential for robust clinical efficacy in BCL-2–dependent tumors without triggering dose-limiting thrombocytopenia.

RESULTS

Structure-based design by a new X-ray complex

The three-dimensional structures of prosurvival proteins in the BCL-2 family such as BCL-2 and BCL-X_L share a common motif comprising two hydrophobic α-helices surrounded by six or seven amphipathic α-helices. Four of these amphipathic helices form a hydrophobic groove approximately 20 Å long that serves as the binding site for proapoptotic proteins[20,21]. As determined by alanine scanning[22], high-affinity binding of proapoptotic peptides to both BCL-2 and BCL-X_L is mediated primarily by interactions in two hydrophobic pockets, termed P2 and P4 (ref. 23), as well as an electrostatic interaction between conserved aspartic acid and arginine residues on the proapoptotic and prosurvival proteins, respectively. Although the core acylsulfonamide moiety of navitoclax does not form direct electrostatic interactions with the conserved arginine, it engages the same two hydrophobic 'hot spots'[24] of BCL-2 and BCL-X_L[21]. As can be seen in the BCL-2–navitoclax X-ray crystal structure, the thiophenyl moiety (**Fig. 1a**) of navitoclax binds in the P4 hot spot of BCL-2 and engages in an intramolecular π-stacking interaction with the tethered arylsulfonamide unit[13,25]. The 1-chloro-4-(4,4-dimethylcyclohex-1-enyl)benzene moiety (**Fig. 1a**) in turn binds deeply within the P2 hot spot[26].

To explore the possibility of imparting BCL-2 selectivity to analogs within the acylsulfonamide class, we reverse engineered navitoclax and related structures through the systematic removal or replacement of key binding elements. This process revealed that analogs lacking the thiophenyl unit (**2**; **Fig. 1b**) were moderately selective for BCL-2, albeit with reduced affinities relative to the parent structures (**Supplementary Table 1**). A subsequent X-ray crystal structure of the BCL-2–**2** complex showed that compound **2** shared a similar global binding motif with navitoclax but occupied a smaller volume within the P4 hot spot. Notably, the complex crystallized as a protein dimer in which a tryptophan side-chain residue (Trp30) from a second BCL-2 protein intercalated into the P4 hot spot of the small molecule–bound protein (**Fig. 1c**). This tryptophan side chain formed an intermolecular π-stacking arrangement with the nitroaryl moiety of compound **2** in a fashion similar to the thiophenyl moiety of navitoclax, thus underscoring the preference for this type of hydrophobic interaction within P4. In addition, the nitrogen atom of the intercalating indole formed a hydrogen bond with Asp103 of BCL-2. This was a key finding, as Asp103 corresponds to Glu96 in BCL-X_L and is one of the few amino acid differences within the BH3-binding domains of the two proteins.

To mimic these interactions, we incorporated a putative P4-binding moiety into the central core of **2** by tethering a 5-substituted indole through an ether linkage (**Supplementary Fig. 1**). An X-ray crystal

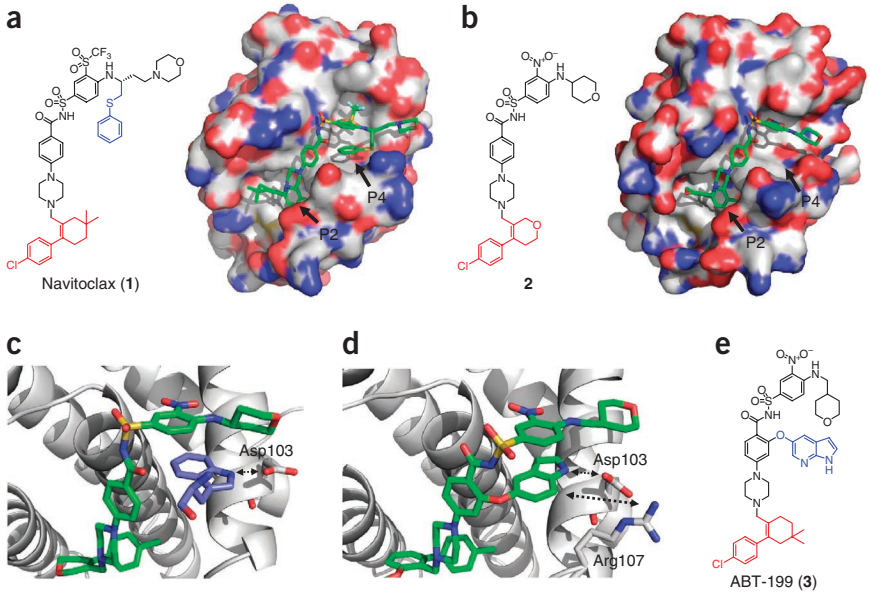

Figure 1 Discovery of ABT-199. (**a**) The 2.05-Å resolution crystal structure of navitoclax (**1**) bound to BCL-2. The protein is shown with a solvent-accessible surface, and carbon atoms are colored orange, oxygen atoms are red and nitrogen atoms are blue (see **Supplementary Table 4** for coordinates). (**b**) The 1.90-Å resolution crystal structure of **2** (4-(4-{[4-(4-chlorophenyl)-5,6-dihydro-2*H*-pyran-3-yl]methyl}piperazin-1-yl)-*N*-{[3-nitro-4-(tetrahydro-2*H*-pyran-4-ylamino)phenyl]sulfonyl}benzamide) bound to BCL-2. The protein is shown with a solvent-accessible surface, and atoms are colored as in **a** (see **Supplementary Table 5** for coordinates). (**c**) Ribbon representation of the complex of BCL-2 with **2**. Arrows indicate the hydrogen bond between Asp103 of BCL-2 and the intercalating indole of Trp30 from a neighboring BCL-2 molecule. (**d**) Ribbon representation of the complex of an indole analog of **2** (see **Supplementary Fig. 1** and **Supplementary Table 6** for coordinates) bound to BCL-2. Arrows indicate the hydrogen bond between Asp103 of BCL-2 and the indole of the ligand and the potential hydrogen bond between Arg107 of BCL-2 and the ligand. (**e**) Chemical structure of ABT-199 (**3**) (4-(4-{[2-(4-chlorophenyl)-4,4-dimethylcyclohex-1-en-1-yl]methyl}piperazin-1-yl)-*N*-({3-nitro-4-[(tetrahydro-2*H*-pyran-4-ylmethyl)amino]phenyl}sulfonyl)-2-(1*H*-pyrrolo[2,3-*b*]pyridin-5-yloxy)benzamide).

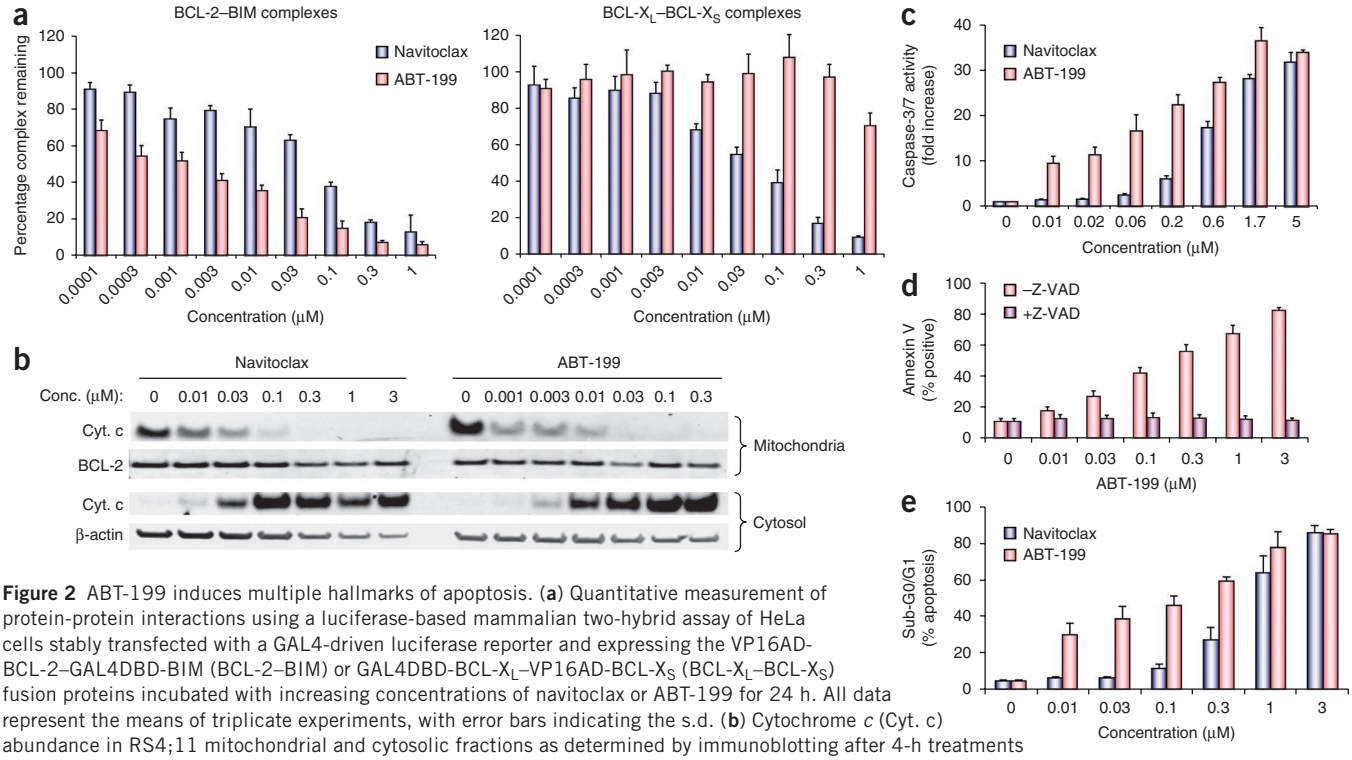

Figure 2 ABT-199 induces multiple hallmarks of apoptosis. (**a**) Quantitative measurement of protein-protein interactions using a luciferase-based mammalian two-hybrid assay of HeLa cells stably transfected with a GAL4-driven luciferase reporter and expressing the VP16AD-BCL-2–GAL4DBD-BIM (BCL-2–BIM) or GAL4DBD-BCL-X_L–VP16AD-BCL-X_S (BCL-X_L–BCL-X_S) fusion proteins incubated with increasing concentrations of navitoclax or ABT-199 for 24 h. All data represent the means of triplicate experiments, with error bars indicating the s.d. (**b**) Cytochrome *c* (Cyt. c) abundance in RS4;11 mitochondrial and cytosolic fractions as determined by immunoblotting after 4-h treatments with increasing concentrations of navitoclax or ABT-199. BCL-2 and β-actin serve as protein loading controls for the mitochondria and cytosol, respectively. Conc., concentration. (**c**) Activation of caspase-3 and caspase-7 (caspase-3/7) in RS4;11 cells after incubation with increasing concentrations of navitoclax or ABT-199 for 4 h. All data represent the mean of triplicate experiments, with error bars indicating the s.e.m. (**d**) Phosphatidylserine exposure as determined by annexin V staining in RS4;11 cells after a 4 h incubation with increasing concentrations of ABT-199 with or without the pan-caspase inhibitor Z-VAD. All data represent the mean of three separate experiments, with error bars indicating the s.e.m. (**e**) Apoptosis (sub-G0/G1 accumulation) as assessed by fluorescence-activated cell sorting (FACS) in RS4;11 cells after incubation with increasing concentrations of ABT-199 or navitoclax for 24 h. All data represent the means of three separate experiments, with error bars indicating the s.e.m.

structure of the resulting molecule bound to BCL-2 (**Fig. 1d**) showed that the tethered indole filled the P4 hot spot and captured the electrostatic interaction with Asp103 in a manner similar to that in the BCL-2–**2** complex (**Fig. 1c**). This core modification also shifted the indole aryl ring toward the basic side chain of Arg107 (**Fig. 1d**), thus offering the possibility of further affinity gains through a second electrostatic interaction. Replacement of the indole with an azaindole as the new P4-binding moiety, along with a structural change in the P2-binding portion (**Fig. 1e**), produced the highly potent and selective compound ABT-199.

ABT-199 cell killing is selective and mechanism dependent

ABT-199 has a subnanomolar affinity for BCL-2 (K_i < 0.010 nM) and bound over three orders of magnitude less avidly to BCL-X_L (K_i = 48 nM) and BCL-W (K_i = 245 nM) than to BCL-2 in a time-resolved fluorescence resonance energy transfer competition binding assay (**Supplementary Table 2**). ABT-199 has no measurable binding to MCL-1 (K_i > 444 nM). To assess selectivity in a cellular context, we tested ABT-199 against interleukin-3 (IL-3)-dependent mouse FL5.12 cells engineered to rely on either BCL-2 (FL5.12–BCL-2 cells) or BCL-X_L (FL5.12–BCL-X_L cells) for survival in the absence of IL-3 (ref. 27). Although ABT-199 potently killed FL5.12–BCL-2 cells (half-maximal effective concentration (EC_{50}) = 4 nM), it showed much weaker activity against FL5.12–BCL-X_L cells (EC_{50} = 261 nM). We found this same selectivity when assessing apoptosis by the accumulation of sub-G0/G1 DNA (**Supplementary Fig. 2**). We also observed cell killing in the BCL-2–dependent acute lymphoblastic leukemia (ALL) cell line RS4;11 (ref. 28) (EC_{50} = 8 nM), whereas BCL-X_L–dependent lines, such as H146 (ref. 29), were more resistant to ABT-199 (EC_{50} = 4,260 nM). ABT-199 also showed selectivity in cellular mammalian two-hybrid assays, where it disrupted BCL-2–BIM complexes (EC_{50} = 3 nM) but was much less effective against BCL-X_L–BCL-X_S (EC_{50} = 2.2 μM; **Fig. 2a**) or MCL-1–NOXA complexes (**Supplementary Fig. 3**). Administration of ABT-199 to RS4;11 cells rapidly induced key hallmarks of apoptosis, including cytochrome *c* release (**Fig. 2b**), caspase activation (**Fig. 2c**), the externalization of phosphatidylserine (**Fig. 2d**) and the accumulation of sub-G0/G1 DNA (**Fig. 2e**). Moreover, cell killing mediated by ABT-199 was caspase dependent, as the addition of the pan-caspase inhibitor Z-VAD completely abrogated its activity (**Fig. 2d**). ABT-199 had no effect on *Bak*$^{-/-}$ *Bax*$^{-/-}$ double knockout mouse embryonic fibroblasts (**Supplementary Fig. 4**), indicating that it probably does not kill cells through an off-target mechanism.

ABT-199 also had single-agent cell-killing activity against a proportion of non-Hodgkin's lymphoma (NHL) cell lines (**Fig. 3a** and **Supplementary Table 3**), including those derived from diffuse large B cell lymphoma (DLBCL), follicular lymphoma or mantle cell lymphoma (MCL), in addition to its activity against acute myelogenous leukemia and ALL lines (**Supplementary Table 3**). Furthermore, NHL cell lines with *BCL2* gains, *BCL2* amplifications or the t(14;18) translocation (together referred to as *BCL2*^{high} cells) were more sensitive to ABT-199 than cell lines without these alterations (P = 0.0018, n = 25 cell lines; **Fig. 3b**). Quantitative immunoblotting revealed that sensitivity to ABT-199 correlated strongly with the expression of BCL-2

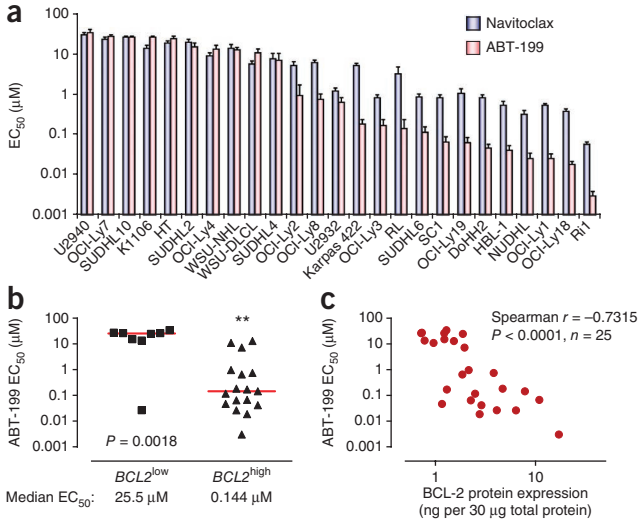

Figure 3 High BCL-2 expression predicts sensitivity to ABT-199 in NHL cell lines. (**a**) Viability of 25 NHL cell lines after incubation with increasing concentrations of navitoclax or ABT-199 for 48 h. All data points represent the mean of at least six experiments, with error bars indicating the s.e.m. Additional details about each cell line, including lymphoma subtype, *BCL2* copy number, presence of t(14;18) and relative expression of BCL-2, BCL-X_L and MCL-1 are provided in **Supplementary Table 3**. (**b**) The EC_{50} values of ABT-199 against cell lines bearing *BCL2* gains, *BCL2* amplifications or the t(14;18) translocation (*BCL2*^{high}) plotted against the values for cell lines without these lesions (*BCL2*^{low}). Red lines indicate the median EC_{50} calculated for each population. *BCL2*^{high} lines were significantly more sensitive to ABT-199 than were *BCL2*^{low} lines (Mann-Whitney test). (**c**) BCL-2 protein expression as assessed by quantitative immunoblotting and plotted against the corresponding ABT-199 EC_{50} for each cell line ($n = 25$ lines). A significant correlation was observed between BCL-2 protein expression and ABT-199 EC_{50} values (Spearman's rank correlation, $P < 0.0001$ by two-tailed t test).

(**Fig. 3c**) but not BCL-X_L (**Supplementary Fig. 5**) across this cell-line panel. *BCL2*^{high} status is thus a potential predictive marker for sensitivity to ABT-199 and may have utility for patient stratification.

Regression of hematological tumors *in vivo*

We evaluated the ability of ABT-199 to suppress tumor growth *in vivo* in a broad spectrum of human hematological tumor xenografts established in immunocompromised mice. After a single oral dose of 12.5 mg per kg body weight in xenografts derived from RS4;11 cells (ALL), ABT-199 caused a maximal tumor growth inhibition (TGI_{max}) of 47% ($P < 0.001$) and tumor growth delay (TGD) of 26% ($P < 0.05$) (**Fig. 4a**). The magnitude and durability of the response increased in a dose-dependent manner, with the highest dose of 100 mg per kg body weight conferring a TGI_{max} of 95% and a TGD of 152% ($P < 0.001$ for both TGI_{max} and TGD). The latter tumor growth inhibition corresponded with an exposure of 78.9 μg h ml^{-1}, which was similar to that achieved with navitoclax in mice[15]. We additionally evaluated ABT-199 in xenografts derived from the Toledo cell line, a model of B cell lymphoma harboring the t(14;18) translocation[30]. Oral administration of 100 mg per kg body weight for 21 d to the mice in this xenograft group significantly inhibited tumor growth compared to vehicle-treated control mice (TGI_{max} = 93%, $P < 0.001$; TGD = 220%, $P < 0.001$; **Fig. 4b**).

In models that were minimally affected by single-agent therapy with a BCL-2 inhibitor, ABT-199 enhanced the efficacy of clinically relevant chemotherapy and immunotherapy. In the DoHH2 xenograft (NHL) model, once a day oral administration of ABT-199 (100 mg per kg body weight) for 14 d inhibited tumor growth (TGI_{max} = 62%, $P < 0.001$; **Fig. 4c**) with marginal durability (TGD = 69%, $P < 0.001$). Although the combination of ABT-199 and rituximab insignificantly ($P = 0.06$) increased the TGI_{max} of rituximab alone, the TGD was increased from 285% with rituximab alone to 408% with

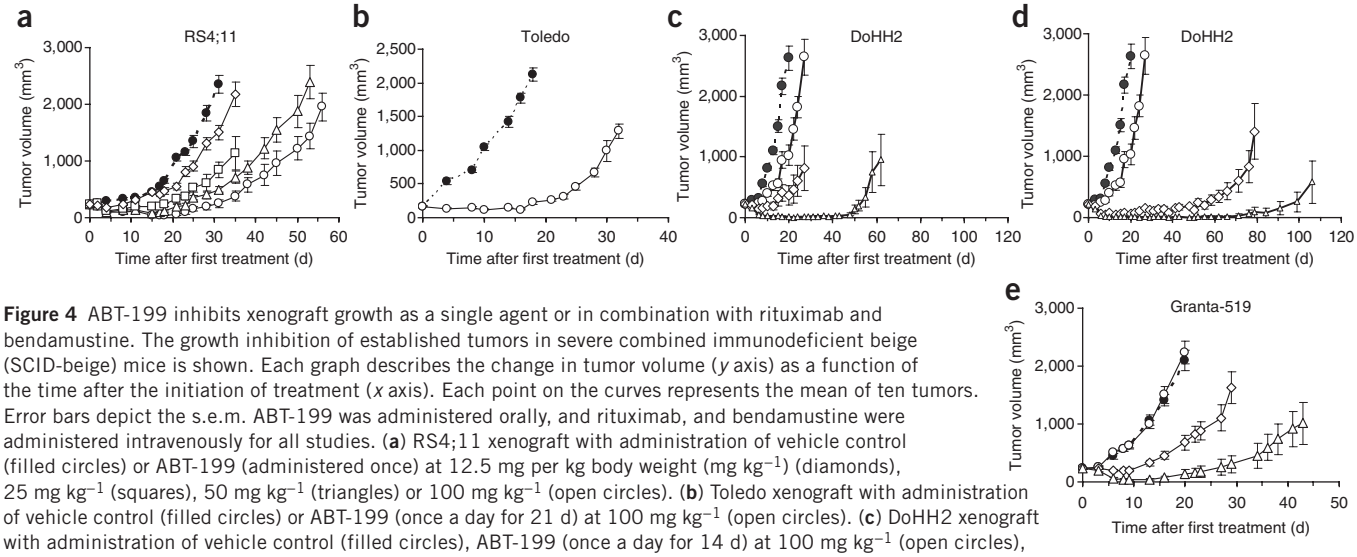

Figure 4 ABT-199 inhibits xenograft growth as a single agent or in combination with rituximab and bendamustine. The growth inhibition of established tumors in severe combined immunodeficient beige (SCID-beige) mice is shown. Each graph describes the change in tumor volume (y axis) as a function of the time after the initiation of treatment (x axis). Each point on the curves represents the mean of ten tumors. Error bars depict the s.e.m. ABT-199 was administered orally, and rituximab, and bendamustine were administered intravenously for all studies. (**a**) RS4;11 xenograft with administration of vehicle control (filled circles) or ABT-199 (administered once) at 12.5 mg per kg body weight (mg kg^{-1}) (diamonds), 25 mg kg^{-1} (squares), 50 mg kg^{-1} (triangles) or 100 mg kg^{-1} (open circles). (**b**) Toledo xenograft with administration of vehicle control (filled circles) or ABT-199 (once a day for 21 d) at 100 mg kg^{-1} (open circles). (**c**) DoHH2 xenograft with administration of vehicle control (filled circles), ABT-199 (once a day for 14 d) at 100 mg kg^{-1} (open circles), rituximab (administered once) at 10 mg kg^{-1} (diamonds) or ABT-199 plus rituximab (triangles). (**d**) DoHH2 xenograft with administration of vehicle control (filled circles), ABT-199 (once a day for 14 d) at 100 mg kg^{-1} (open circles), the combination (administered once) of bendamustine at 25 mg kg^{-1} and rituximab at 10 mg kg^{-1} (diamonds) or ABT-199 plus the bendamustine and rituximab combination (triangles). (**e**) Granta-519 xenograft with administration of vehicle control (filled circles), ABT-199 (once a day for 3 d) at 33 mg kg^{-1} (open circles), the bendamustine and rituximab combination (diamonds) or ABT-199 plus the bendamustine and rituximab combination (triangles). For the experiment in **e**, the bendamustine and rituximab combination was administered as two daily doses of bendamustine at 12.5 mg kg^{-1} and a single dose of rituximab at 10 mg kg^{-1}. For the dose-response curves of ABT-199 as a single agent in the Toledo xenograft model and in combination with bendamustine plus rituximab in the Granta-519 model, see **Supplementary Figure 8**.

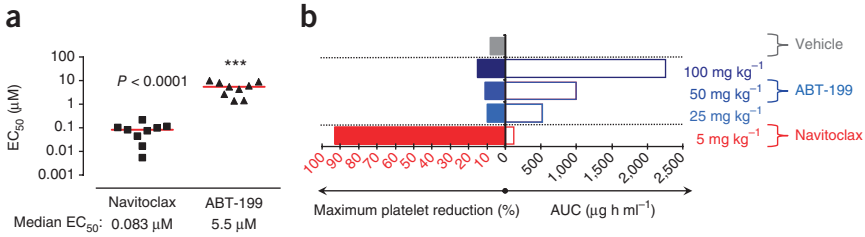

Figure 5 ABT-199 shows reduced effects on platelets compared to navitoclax. (**a**) The EC_{50} values of navitoclax and ABT-199 against platelets from matched human donors. Filled squares (navitoclax) and triangles (ABT-199) designate individual donor samples. Red lines indicate the median EC_{50} calculated for each population. ABT-199 was significantly less potent against human platelets than navitoclax in matched donor samples (Mann-Whitney test; $***P < 0.0001$ for comparisons between the ABT-199 and navitoclax groups (two-tailed *t* test); $n = 9$ donor samples per group). (**b**) The effect of navitoclax (5 mg per kg body weight (mg kg^{-1}) orally) and ABT-199 (25, 50 or 100 mg kg^{-1} orally) on circulating platelets in dogs that received a single oral dose of navitoclax ($n = 3$) or ABT-199 ($n = 2$ for the 25 mg kg^{-1} and 50 mg kg^{-1} doses, and $n = 1$ for the 100 mg kg^{-1} dose) in the quantities indicated (*y* axis). The maximum reduction in the number of platelets within a period of 24 h is shown (*x* axis, left), as well as the plasma exposure (*x* axis, right). Plasma exposures are expressed as μg h ml^{-1} over 24 h, and the maximum reduction in platelet count was assessed from baseline at $t = 0$ h.

the combination ($P < 0.001$). This combination induced complete responses (tumors ≤25 mm^3 for at least three consecutive measurements) in 100% of the mice, whereas no mice had a complete response after treatment with either rituximab or ABT-199 alone. The combination of a single intravenous dose of bendamustine[31] at 25 mg per kg body weight with rituximab plus ABT-199 further enhanced the durability of the response (TGD = 977%, $P < 0.001$; **Fig. 4d**). In mice bearing established Granta-519 (MCL) tumors, three consecutive oral doses of ABT-199 (33 mg per kg body weight once a day) enhanced the TGD (**Fig. 4e**) induced by the combination of bendamustine and rituximab[31] from 108% to 258% ($P < 0.001$) and caused a complete response in 50% of the mice, whereas no mice had a complete response after treatment with the bendamustine plus rituximab combination alone. These data indicate that continuous administration of ABT-199 may not be necessary to gain optimal efficacy when combined with bendamustine and rituximab. Throughout these studies, all treatments with ABT-199 alone or in combination were well tolerated in mice without overt signs of toxicity or weight loss >8% (**Supplementary Fig. 6**).

ABT-199 is platelet sparing and reduces CLL tumor burden

We tested our hypothesis that a BCL-2–selective inhibitor would spare platelets by evaluating the effects of navitoclax and ABT-199 on human platelets *ex vivo*. Although navitoclax potently killed human platelets (average $EC_{50} = 0.083$ μM), ABT-199 was substantially less active ($EC_{50} = 5.5$ μM; **Fig. 5a**). The preclinical thrombocytopenia caused by navitoclax was further exemplified by the rapid platelet decrease after oral administration in dogs, where a single 5 mg per kg body weight oral dose reduced the number of circulating platelets by 95% from baseline within 6 h (area under the curve (AUC) = 115 μg h ml^{-1}; **Fig. 5b**). In contrast, single oral doses of ABT-199 as high as 100 mg per kg body weight resulted in substantial plasma concentrations (AUC = 2,261 μg h ml^{-1}) relative to a highly efficacious plasma exposure in mice while having minimal effects on the number of circulating platelets. Thus, selective inhibition of BCL-2 by ABT-199 has markedly reduced effects on platelets both *ex vivo* and *in vivo* compared to navitoclax.

The susceptibility of CLL to BCL-2 inhibition[16,17] is associated with the high expression of this protein in patient-derived peripheral blood samples[32,33]. We therefore investigated whether the *in vitro* cytotoxicity of ABT-199 extended to primary samples of CLL cells. In all 15 specimens, ABT-199 induced concentration-dependent apoptosis with an average EC_{50} of 3.0 nM (**Fig. 6a**). To translate these findings into the clinical setting, we initiated a first-in-human trial in patients with refractory CLL. The initial cohort ($n = 3$) received a dose of ABT-199 on day −3 for an evaluation of pharmacokinetics and safety and then followed a continuous daily dosing regimen starting on day 1. Notably, a single dose of ABT-199 (200 mg or 100 mg)

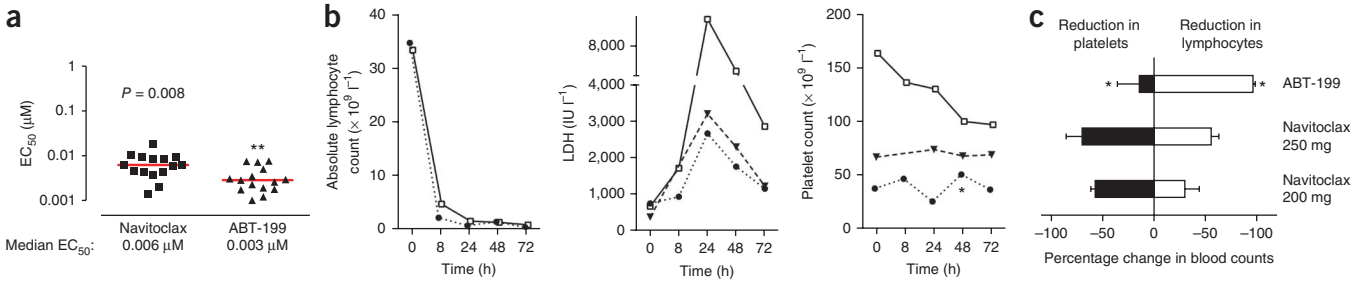

Figure 6 Efficacy of ABT-199 treatment against CLL cells *in vitro* and *in vivo*. (**a**) The EC_{50} values of ABT-199 (triangles) and navitoclax (squares) for *in vitro* killing of peripheral blood CLL cells collected from subjects with CLL. Red lines indicate the median EC_{50}. ABT-199 was more potent than navitoclax in matched CLL samples (Mann-Whitney; $**P < 0.01$ for comparisons between the ABT-199 and navitoclax groups (two-tailed *t* test); $n = 15$ samples per group). (**b**) Changes in circulating lymphocyte count (left), LDH (middle) and platelet count (right) in the first three patients entered into the first-in-human clinical trial, with each patient receiving a single oral dose of ABT-199, either 200 mg (patients 101 (triangles) and 103 (circles)) or 100 mg (patient 104 (squares)). No lymphocyte data for patient 101 is shown, as circulating CLL cells were undetectable in this patient at study entry. For lymphocyte count, the upper limit of the normal range is 4.0×10^9 l^{-1}; for LDH, the upper limit of the normal range is 450 IU l^{-1}; and for platelet count, the lower limit of the reference range is 140×10^9 l^{-1}. The asterisk indicates a platelet transfusion in the 24-h period before this count. (**c**) Comparison of the effects after 24 h of a single dose of ABT-199 or navitoclax on platelet and lymphocyte counts in patients normalized to their baseline count. The ABT-199 data are the same as in **b**, and the navitoclax data are from a clinical trial described elsewhere[17]. $n = 3$ patients per cohort. For the ABT-199 and navitoclax 200-mg cohorts, the lymphocyte data only include results for patients with baseline lymphocytosis ($n = 2$). The mean and s.d. are plotted. $*P < 0.05$ for comparisons between the ABT-199 and navitoclax groups (analysis of variance and Student-Newman-Keuls test).

resulted in a rapid reduction in palpable lymphadenopathy within 24 h and a >95% reduction in peripheral blood lymphocytosis in the two subjects with pretreatment lymphocytosis (**Fig. 6b**). Serial serum biochemistry studies in all three patients showed tumor lysis with marked increases in serum lactate dehydrogenase (LDH; **Fig. 6b**) and phosphate (data not shown) concentrations, as seen when the rate of release of tumor cell–breakdown products overwhelms the excretory mechanisms of the body[34]. Patients experienced minor symptoms only and had no major organ dysfunction, although one patient (103) developed mild disseminated intravascular coagulation as a consequence of the tumor lysis. This patient experienced an exacerbation of major pre-existing CLL-related thrombocytopenia that recovered to baseline when the disseminated intravascular coagulation resolved (**Fig. 6b**) and did not recur with subsequent longer-term re-exposure to drug (**Supplementary Fig. 7**). The remaining patients showed negligible (patient 101) or clinically unsubstantial (patient 104) decreases in their platelet numbers. The effects on platelet counts in these three patients were minor compared with the acute thrombocytopenia observed when similar patients were treated with navitoclax in previous trials[16,17] (**Fig. 6c**). In sharp contrast, ABT-199 induced a much greater immediate antileukemic effect than that previously observed with single doses of navitoclax, consistent with preclinical predictions.

DISCUSSION

CLL and NHL are among the most common cancers in the United States, with an estimated 66,360 and 14,570 new cases, respectively, diagnosed in 2011 (ref. 35). Although some lymphomas and CLL can be effectively treated with combinations of chemotherapy and immunotherapy, many patients eventually become refractory to these treatments and ultimately succumb to their disease[36]. Consequently, there is a substantial need for new therapies that can improve on current treatment options. One area that has garnered considerable interest in recent years is the generation of therapies that can restore apoptosis to tumors by directly targeting the BCL-2 family of proteins.

The role of BCL-2 in the survival of lymphoid malignancies is well established, and its overexpression is driven by various mechanisms. For example, the t(14;18) chromosome translocation breakpoint is the defining genetic aberration in B cell follicular lymphoma[4,5] and is also found in approximately 30% of DLBCL[8], the largest subgroup of NHL[37]. This translocation brings the *BCL2* gene under control of the immunoglobulin heavy chain enhancer, resulting in high BCL-2 expression. Amplification of the chromosome region 18q21, where the *BCL2* gene resides, is common in both MCL and the activated B cell subtype of DLBCL, where it negatively correlates with overall survival[38]. BCL-2 is also overexpressed in acute[39,40] and chronic (CLL[32,33,41]) leukemias, the latter of which often lack the microRNAs miR-15a and miR-16-1 that negatively regulate BCL-2 expression[42,43].

Navitoclax, a first-in-class orally bioavailable BCL-2 family inhibitor, has shown efficacy in patients with refractory CLL. This agent was designed as a dual inhibitor of both BCL-2 and BCL-X_L, and inhibition of the latter protein induces a concentration-dependent thrombocytopenia that is dose limiting in the clinic. We hypothesized that achieving greater efficacy in BCL-2–dependent tumors would require the development of a BCL-2 family inhibitor lacking the dose-limiting thrombocytopenia caused by inhibition of BCL-X_L. However, the generation of selective BCL-2 inhibitors is a considerable challenge because of the high degree of similarity within the BH3-binding domains of BCL-2 and BCL-X_L. Further, although peptides have been engineered for high affinity and selectivity for BCL-X_L[44], the successful design of a truly BCL-2–selective peptide has not been achieved. In the course of our efforts, we discovered a unique BCL-2–complex crystal packing that afforded insights into the redesign of navitoclax. Specifically, the X-ray crystal structure of a dimeric BCL-2–**2** complex suggested an alternative attachment point for the crucial P4-binding moiety, along with an additional means of generating selective and high-affinity binding through an electrostatic interaction favoring BCL-2. These structural cues led to the design and generation of ABT-199, a potent BCL-2 inhibitor with substantially lower binding affinity toward BCL-X_L. Consistent with its lower BCL-X_L inhibition, ABT-199 spared human platelets *ex vivo* as compared to navitoclax. Additionally, higher concentrations of ABT-199 relative to preclinical efficacy exposures were achieved in dogs without a substantial impact on circulating platelets.

ABT-199 induced apoptosis in hematological cancer cell lines that rely on BCL-2 for survival and showed potent cell killing against primary CLL samples. Additionally, tumor regression was achieved with ABT-199 as a single agent or in combination with relevant chemotherapy or immunotherapy across four mouse xenograft models without substantial weight loss or signs of general malaise. Administration of a single dose of ABT-199 induced rapid tumor lysis in the first three patients with refractory CLL treated in the first-in-human clinical trial, thereby ultimately establishing specific BCL-2 inhibition as a valid approach for cancer therapy. To mitigate the risks of tumor lysis in subsequent patients, the starting dose was reduced to 50 mg, and continuous dosing was escalated weekly in a stepwise fashion to the targeted daily dose[45]. A comparison of the effects of single doses of ABT-199 and navitoclax in patients with CLL in separate trials revealed more potent antileukemic activity for ABT-199, as well as less antiplatelet activity and a more favorable therapeutic index.

The ability to identify potential responders to new cancer therapeutics is a crucial aspect of targeted therapy[46]. Profiling the activity of ABT-199 against a number of diverse NHL cell lines has identified *BCL2* gains, *BCL2* amplification or the presence of the t(14;18) translocation as indicators of sensitivity to this agent. These lesions are readily assessed by available diagnostic tools and are thus potential strategies for patient selection in the clinical setting.

ABT-199 is a first-in-class orally bioavailable BCL-2–selective inhibitor that shows potent cell killing *in vitro* and antitumor efficacy *in vivo*. The lack of BCL-X_L inhibition with ABT-199 should allow for higher circulating concentrations of the drug to be achieved in patients with cancer without dose-limiting thrombocytopenia. This hypothesis is being formally tested in an ongoing phase 1 study[45]. Furthermore, the role of BCL-2 in multiple hematological malignancies suggests that ABT-199 could be effective as a single agent or in combination with conventional therapies across a breadth of associated diseases, and it therefore has the potential to shift current treatment paradigms in hematological cancers.

METHODS

Methods and any associated references are available in the online version of the paper.

Note: Supplementary information is available in the online version of the paper.

ACKNOWLEDGMENTS

We thank M. Bruncko, E. Fry, L. Hasvold, L. Hexamer, A. Kunzer, A. Petros, X. Song, Z. Tao, L. Wang and X. Wang for contributions to the generation of ABT-199 and related analogs and J. Bouska, and D. Osterling for analytical support. The authors acknowledge G. Chiang and A. Vasudevan for critical reading of this manuscript, L. Belmont, I. Wertz, J. Adams, S. Cory, P. Colman, P. Czabotar and G. Lessene for useful discussions and K. Lowes, E. Litvinovich and L. Roberts

for technical analysis. Research performed at the Walter and Eliza Hall Institute (WEHI) was supported by grants and fellowships from the Australian National Health and Medical Research Council (NHMRC, including an Independent Research Institutes Infrastructure Support Scheme (IRIISS) grant), the Australian Cancer Research Foundation, the Leukaemia Foundation of Australia, the Cancer Council of Victoria, the Victorian Cancer Agency, the Victorian State Government Operational Infrastructure Support and the Leukemia Lymphoma Society.
The authors acknowledge L.M. Staudt (US National Institutes of Health) for DLBCL cell lines.

AUTHOR CONTRIBUTIONS

A.J.S., S.W.E., S.H.R., S.G.H., W.J.F., D.C.S.H., J.D.L. and C.T. directed aspects of the preclinical research. A.J.S. and J.D.L. interpreted data and wrote the manuscript. A.W.R., S.H.E., J.F.S. and R.A.H. directed the clinical trial design, generated patient data and interpreted results, and A.W.R. contributed in writing the manuscript. S.L.K. generated *in vitro* CLL experiments. K.D.M. generated *in vitro* normal volunteer platelet data. M.J.M., E.R.B., S.L.A., D.S., H.L.M., J.L. and A.O. generated *in vivo* pharmacology data, and E.R.B. contributed in writing of the manuscript. M.D.W., C.-M.P., G.M.S., H.D. and A.J.S. conceived of or generated the compounds described in the manuscript. C.H.P. generated the X-ray structures. J.D.L., D.C.P., S.J., S.K.T., J.C., J.C.X., P.M.N., Y.X., H.Z., P.J.K., C.T., L.T.L. and M.L.S. performed the biological characterization of ABT-199 and other compounds described in the manuscript. N.D.C., B.D.D. and K.C.M. generated the pharmacokinetic and platelet data in conscious dogs.

COMPETING FINANCIAL INTERESTS

The authors declare competing financial interests: details are available in the online version of the paper.

Published online at http://www.nature.com/doifinder/10.1038/nm.3048.
Reprints and permissions information is available online at http://www.nature.com/reprints/index.html.

1. Hanahan, D. & Weinberg, R.A. The hallmarks of cancer. *Cell* **100**, 57–70 (2000).
2. Adams, J.M. & Cory, S. The Bcl-2 apoptotic switch in cancer development and therapy. *Oncogene* **26**, 1324–1337 (2007).
3. Youle, R.J. & Strasser, A. The BCL-2 protein family: opposing activities that mediate cell death. *Nat. Rev. Mol. Cell Biol.* **9**, 47–59 (2008).
4. Tsujimoto, Y., Cossman, J., Jaffe, E. & Croce, C.M. Involvement of the bcl-2 gene in human follicular lymphoma. *Science* **228**, 1440–1443 (1985).
5. Cleary, M.L., Smith, S.D. & Sklar, J. Cloning and structural analysis of cDNAs for bcl-2 and a hybrid bcl-2/immunoglobulin transcript resulting from the t(14;18) translocation. *Cell* **47**, 19–28 (1986).
6. Boise, L.H. *et al.* Bcl-x, a bcl-2–related gene that functions as a dominant regulator of apoptotic cell death. *Cell* **74**, 597–608 (1993).
7. Vaux, D.L., Cory, S. & Adams, J.M. *Bcl-2* gene promotes haemopoietic cell survival and cooperates with c-myc to immortalize pre-B cells. *Nature* **335**, 440–442 (1988).
8. Huang, J.Z. *et al.* The t(14;18) defines a unique subset of diffuse large B-cell lymphoma with a germinal center B-cell gene expression profile. *Blood* **99**, 2285–2290 (2002).
9. Minn, A.J., Rudin, C.M., Boise, L.H. & Thompson, C.B. Expression of bcl-xl can confer a multidrug resistance phenotype. *Blood* **86**, 1903–1910 (1995).
10. Amundson, S.A. *et al.* An informatics approach identifying markers of chemosensitivity in human cancer cell lines. *Cancer Res.* **60**, 6101–6110 (2000).
11. Zhang, H. *et al.* Bcl-2 family proteins are essential for platelet survival. *Cell Death Differ.* **14**, 943–951 (2007).
12. Mason, K.D. *et al.* Programmed anuclear cell death delimits platelet life span. *Cell* **128**, 1173–1186 (2007).
13. Oltersdorf, T. *et al.* An inhibitor of Bcl-2 family proteins induces regression of solid tumours. *Nature* **435**, 677–681 (2005).
14. Park, C.M. *et al.* Discovery of an orally bioavailable small molecule inhibitor of prosurvival B-cell lymphoma 2 proteins. *J. Med. Chem.* **51**, 6902–6915 (2008).
15. Tse, C. *et al.* ABT-263: a potent and orally bioavailable Bcl-2 family inhibitor. *Cancer Res.* **68**, 3421–3428 (2008).
16. Wilson, W.H. *et al.* Navitoclax, a targeted high-affinity inhibitor of BCL-2, in lymphoid malignancies: a phase 1 dose-escalation study of safety, pharmacokinetics, pharmacodynamics, and antitumour activity. *Lancet Oncol.* **11**, 1149–1159 (2010).
17. Roberts, A.W. *et al.* Substantial susceptibility of chronic lymphocytic leukemia to BCL2 inhibition: results of a phase I study of navitoclax in patients with relapsed or refractory disease. *J. Clin. Oncol.* **30**, 488–496 (2012).
18. Gandhi, L. *et al.* Phase I study of Navitoclax (ABT-263), a novel Bcl-2 family inhibitor, in patients with small-cell lung cancer and other solid tumors. *J. Clin. Oncol.* **29**, 909–916 (2011).
19. Petros, A.M. *et al.* Solution structure of the antiapoptotic protein bcl-2. *Proc. Natl. Acad. Sci. USA* **98**, 3012–3017 (2001).
20. Muchmore, S.W. *et al.* X-ray and NMR structure of human Bcl-xL, an inhibitor of programmed cell death. *Nature* **381**, 335–341 (1996).
21. Wendt, M.D. Discovery of ABT-263, a Bcl-family protein inhibitor: observations on targeting a large protein-protein interaction. *Expert Opin. Drug. Discov.* **3**, 1123–1143 (2008).
22. Sattler, M. *et al.* Structure of Bcl-xL-Bak peptide complex: recognition between regulators of apoptosis. *Science* **275**, 983–986 (1997).
23. Lee, E.F. *et al.* Crystal structure of ABT-737 complexed with Bcl-xL: implications for selectivity of antagonists of the Bcl-2 family. *Cell Death Differ.* **14**, 1711–1713 (2007).
24. Atwell, S., Ultsch, M., De Vos, A.M. & Wells, J.A. Structural plasticity in a remodeled protein-protein interface. *Science* **278**, 1125–1128 (1997).
25. Wendt, M.D. *et al.* Discovery and structure-activity relationship of antagonists of B-cell lymphoma 2 family proteins with chemopotentiation activity *in vitro* and *in vivo*. *J. Med. Chem.* **49**, 1165–1181 (2006).
26. Bruncko, M. *et al.* Studies leading to potent, dual inhibitors of Bcl-2 and Bcl-xL. *J. Med. Chem.* **50**, 641–662 (2007).
27. Harada, H., Quearry, B., Ruiz-Vela, A. & Korsmeyer, S.J. Survival factor–induced extracellular signal-regulated kinase phosphorylates BIM, inhibiting its association with BAX and proapoptotic activity. *Proc. Natl. Acad. Sci. USA* **101**, 15313–15317 (2004).
28. Del Gaizo Moore, V., Schlis, K.D., Sallan, S.E., Armstrong, S.A. & Letai, A. BCL-2 dependence and ABT-737 sensitivity in acute lymphoblastic leukemia. *Blood* **111**, 2300–2309 (2008).
29. Shoemaker, A.R. *et al.* Activity of the Bcl-2 family inhibitor ABT-263 in a panel of small cell lung cancer xenograft models. *Clin. Cancer Res.* **14**, 3268–3277 (2008).
30. Singh, R.R. *et al.* Hedgehog signaling pathway is activated in diffuse large B-cell lymphoma and contributes to tumor cell survival and proliferation. *Leukemia* **24**, 1025–1036 (2010).
31. Ackler, S. *et al.* Navitoclax (ABT-263) and bendamustine ± rituximab induce enhanced killing of non-Hodgkin's lymphoma tumors *in vivo*. *Br. J. Pharmacol.* **167**, 881–891 (2012).
32. Marschitz, I. Analysis of Bcl-2 protein expression in chronic lymphocytic leukemia. *Am. J. Clin. Pathol.* **113**, 219–229 (2000).
33. Samuel, S. *et al.* VSV oncolysis in combination with the BCL-2 inhibitor obatoclax overcomes apoptosis resistance in chronic lymphocytic leukemia. *Mol. Ther.* **18**, 2094–2103 (2010).
34. Rampello, E., Fricia, T. & Malaguarnera, M. The management of tumor lysis syndrome. *Nat. Clin. Pract. Oncol.* **3**, 438–447 (2006).
35. American Cancer Society. *Cancer Facts &* Figures 2011. <http://www.cancer.org/acs/groups/content/@epidemiologysurveilance/documents/document/acspc-029771.pdf> (2011).
36. Sawas, A., Diefenbach, C. & O'Connor, O.A. New therapeutic targets and drugs in non-Hodgkin's lymphoma. *Curr. Opin. Hematol.* **18**, 280–287 (2011).
37. Bea, S. *et al.* Diffuse large B-cell lymphoma subgroups have distinct genetic profiles that influence tumor biology and improve gene-expression based survival prediction. *Blood* **106**, 3183–3190 (2005).
38. Iqbal, J. *et al.* BCL2 expression is a prognostic marker for the activated B-cell–like type of diffuse large B-cell lymphoma. *J. Clin. Oncol.* **24**, 961–968 (2006).
39. Irish, J.M. *et al.* Flt3 Y591 duplication and Bcl-2 overexpression are detected in acute myeloid leukemia cells with high levels of phosphorylated wild-type p53. *Blood* **109**, 2589–2596 (2007).
40. Coustan-Smith, E. *et al.* Clinical relevance of BCL-2 overexpression in childhood acute lymphoblastic leukemia. *Blood* **87**, 1140–1146 (1996).
41. Campàs, C. *et al.* Bcl-2 inhibitors induce apoptosis in chronic lymphocytic leukemia cells. *Exp. Hematol.* **34**, 1663–1669 (2006).
42. Cimmino, A. *et al.* MiR-15 and miR-16 induce apoptosis by targeting BCL2. *Proc. Natl. Acad. Sci. USA* **102**, 13944–13949 (2005).
43. Calin, G.A. *et al.* MiR-15a and miR-16–1 cluster functions in human leukemia. *Proc. Natl. Acad. Sci. USA* **105**, 5166–5171 (2008).
44. Matsumura, N. *et al.* mRNA display selection of a high-affinity, Bcl-X(L)-specific binding peptide. *FASEB J.* **24**, 2201–2210 (2010).
45. Roberts, A.W. *et al.* Selective inhibition of BCL-2 is active against chronic lymphocytic leukemia (CLL): first clinical experience with the BH3-mimetic ABT-199. Abstract 546 (European Hematology Association 2012, Amsterdam, The Netherlands, June 14–17, 2012).
46. La Thangue, N.B. & Kerr, D.J. Predictive biomarkers: a paradigm shift towards personalized cancer medicine. *Nat. Rev. Clin. Oncol.* **8**, 587–596 (2011).

ONLINE METHODS

Binding affinity assays. Fluorescence polarization binding affinity assays were performed for BCL-2 and BCL-X_L as previously described for BCL-X_L[47]. Time-resolved fluorescence resonance energy transfer binding affinity assays were performed for BCL-2, BCL-X_L and MCL-1 as previously described for BCL-X_L[15].

Antibodies. Antibodies used for quantitative immunoblots were to the following: BCL-2 (BD Transduction Laboratories, 7/Bcl-2, 1:1,000), BCL-X_L (BD Transduction Laboratories, 4, 1:1,000) and MCL-1 (Santa Cruz, S-19, 1:1,000). Cytochrome *c* (BD Biosciences, 7H8.2C12, 1:1,000) and β-actin (Abcam, AC-15, 1:5,000) immunoblots were performed with mouse monoclonal antibodies.

Mechanism-of-action studies. To determine whether ABT-199 induced cell death through on-target intrinsic apoptosis, we performed a series of assays designed to assess multiple and sequential events that occur during programmed cell death. To first determine whether cytochrome *c* was released in RS4;11 cells after treatment with apoptosis-inducing agents, 1×10^6 cells were treated for 4 h (37 °C, 5% CO_2) with navitoclax or ABT-199 (half-log dilutions starting at 3.0 μM and ending at 0.01 μM). Cells were then processed as described previously[48]. To assess caspase-3/7 activation, RS4;11 cells were seeded into 96-well plates at 5,000 cells per well, and navitoclax or ABT-199 was added in half-log dilutions starting at 5 μM and ending at 0.01 μM. The cells were then incubated at 37 °C (5% CO_2) for 3.5 h before being left at room temperature for another 0.5 h. Caspase-3/7 activity was assessed using the Caspase-GLO kit (Promega). The externalization of phosphatidylserine as determined through annexin V staining was performed as follows: RS4;11 cells were seeded into T-25 tissue culture flasks at 2×10^6 ml^{-1} in RPMI 1640 medium (Invitrogen) supplemented with 10% human serum (Sigma) with or without 100 μM Z-VAD. After a 1-h incubation, cells were plated into 48-well tissue culture plates at 4×10^5 per well. The cells were then treated for 4 h with ABT-199 in half-log dilutions starting at 3.0 μM and ending at 0.01 μM (400 μl total volume) in duplicate. For each sample, all of the cells from the well were transferred to a 12 mm × 75 mm culture tube before adding 1 ml of Dulbecco's phosphate-buffered saline (D-PBS) (Invitrogen). The tubes were centrifuged, the supernatant was removed and the cells were gently re-suspended. After the wash, 100 μl of annexin V–binding buffer (BD Pharmingen) were added to all samples except the controls, to which 100 μl of D-PBS were added. The samples were incubated at room temperature in the dark for 15 min with 5 μl of annexin V Alexa Fluor 647 (Invitrogen, A23204, 1:20) before being analyzed on a FACSCalibur. After treatment with ABT-199 or navitoclax, we performed an analysis of the percentage of cells in sub-G0/G1 by FACS. RS4;11 cells were incubated with increasing concentrations of ABT-199 or navitoclax for 24 h. The percentage of apoptotic cells was determined by flow cytometric analysis of the sub-G0/G1 DNA population in cell-cycle histograms as described in detail elsewhere[49]. FL5.12 cells were treated with a single concentration of ABT-199 or navitoclax for 24 h and assessed in the same manner.

Mammalian two-hybrid assay. HeLa cells stably expressing a GAL4-luciferase reporter were seeded into 10-cm dishes at 5×10^5 cells per plate. Twenty-four micrograms of a plasmid expressing both the 'bait' and 'prey' fusion proteins (GAL4DBD-BIM and VP16AD–BCL-2, GAL4DBD–BCL-X_L and VP16AD–BCL-X_S, or GAL4DBD–MCL-1 and VP16AD-NOXA, respectively) were mixed with 1.5 ml OptiMEM (Invitrogen). Separately, 24 μl Lipofectamine 2000 (Invitrogen) were mixed with 1.5 ml OptiMEM. Both solutions were incubated for 5 min at room temperature and then mixed together for 20 min. Three milliliters of the mixture were added to cells in 12 ml culture medium lacking antibiotics, incubated at 37 °C for 24 h and then transferred to 96-well plates at 20,000 cells per well. Compounds were added in half-log dilutions starting from 1 μM and ending at 0.0001 μM for 24 h, and luciferase activity was assessed using ONE-Glo reagent (Promega). All data were plotted as the percentage of complex remaining relative to untreated controls.

Cell lines. NHL cell lines were maintained in Iscove's Modified Dulbecco's Medium (IMDM; Invitrogen) supplemented with 10% human AB serum (Sigma). All other cell lines were acquired from American Type Culture Collection (ATCC; Manassas, VA) and maintained according to their recommendations.

Cell proliferation and viability assays. RS4;11 cells were seeded at 50,000 per well in 96-well plates and treated with compounds diluted in half-log steps starting at 1 μM and ending at 0.00005 μM. All other leukemia and lymphoma cell lines were seeded at 15,000–20,000 cells per well in the appropriate medium and incubated with ABT-199 or navitoclax for 48 h. Effects on proliferation were determined using Cell TiterGlo reagent (Promega). EC_{50} values were determined by nonlinear regression analysis of the concentration-response data. Mouse FL5.12–BCL-2 and FL5.12–BCL-X_L cells were propagated and assessed as described previously[4]. *Bak*$^{-/-}$ *Bax*$^{-/-}$ double knockout mouse embryonic fibroblasts were seeded into 96-well microtiter plates at 5,000 cells per well in DMEM supplemented with 10% FBS. ABT-199 in the same culture medium was added in half-log dilutions starting at 5 μM. The cells were then incubated at 37 °C (5% CO_2) for 48 h, and the effects on proliferation were determined using Cell TiterGlo reagent (Promega) according to the manufacturer's instructions.

***In vivo* xenograft trials.** We conducted all animal studies in accordance with the guidelines approved by the Institutional Animal Care and Use Committees of AbbVie or Genentech. Female C.B-17 SCID mice (DoHH2 and Granta-519 xenografts) and female C.B-17 SCID-beige mice (RS4;11 and Toledo xenografts) (Charles River Laboratories) were inoculated with 1×10^6 (DoHH2) or 5×10^6 (Granta-519, Toledo and RS4;11) cells subcutaneously in the right flank. The inoculation volume (0.2 ml) comprised a 50:50 mixture of cells in growth media and Matrigel (BD Biosciences). Electronic calipers were used to measure the length and width of each tumor 2–3 times per week. Tumor volume was estimated by applying the following equation: volume = length × width^2/2. When tumors reached approximately 220 mm^3, mice were size matched (day 0) into treatment and control groups. All xenograft trials were conducted using ten mice per group, and all mice were ear tagged and monitored individually throughout the studies. ABT-199 was formulated for oral dosing in 60% phosal 50 propylene glycol (PG), 30% polyethylene glycol (PEG) 400 and 10% ethanol, and bendamustine and rituximab were formulated in accordance with the manufacturer's instructions. Drug doses and regimens were administered as described in **Figure 4**. ABT-199 was delivered approximately 2 h before bendamustine or bendamustine plus rituximab. TGI_{max} was calculated as the greatest treatment response using the following equation: TGI_{max} = (1 − mean tumor volume of the treated group/mean tumor volume of the vehicle control group) × 100. The TGD (%) was determined as the percentage increase of the median time period for the treatment group to reach an arbitrary tumor volume of 1,000 mm^3 relative to the vehicle control group. A complete tumor regression response was the portion of the population with tumors ≤25 mm^3 for at least three consecutive measurements. Statistical significance within the experiments for TGI_{max} and TGD were performed by Student's *t* test and Wilcoxon rank sum, respectively. Significance for complete response was performed by two-tailed Fisher's exact test.

***Ex vivo* viability assays.** The Human Research Ethics Committee (HREC) of the Walter and Eliza Hall Institute approved conduct of *ex vivo* assays with donated human cells. Peripheral blood samples from subjects with CLL were collected with informed consent under approval from the Melbourne Health HREC. Mononuclear cells were incubated for 24 h in IMDM plus 10% FCS with titrated concentrations of navitoclax or ABT-199 ranging from 1 nM to 1,000 nM. Viable CLL cells were enumerated by flow cytometry using beads (Calibrite) with concurrent propidium iodide exclusion and surface staining of CD5 and CD19, as described previously[50]. Concentration response curves were fitted using GraphPad Prism to determine EC_{50} values. Platelets suspended in plasma were collected by apheresis from volunteer donors after obtaining written consent (Australian Red Cross Blood Transfusion Service). After dilution 1:10 in Tyrode's buffer, platelets were incubated for 24 h at 37 °C with graduated concentrations of test drugs dissolved in DMSO. Control wells included plasma, no drug and DMSO only. At 24 h, viability was assessed using the Cell TiterGlo assay (Promega). Luminescence was normalized to the no-drug well (100% viability). The EC_{50} was calculated using GraphPad Prism software.

Canine platelet studies. We evaluated the *in vivo* platelet response to navitoclax and ABT-199 in beagle dogs obtained from an established in-house colony. The dogs (both genders) were fasted overnight with free access to water. Food was provided to the dogs either 30 min before (ABT-199) or 12 h after (navitoclax) dosing. Groups of dogs received a 5 mg per kg body weight oral dose of navitoclax ($n = 3$) or 25 mg per kg body weight ($n = 2$), 50 mg per kg body weight ($n = 2$) or 100 mg per kg body weight ($n = 1$) oral doses of ABT-199. Both compounds were administered as a solution in a lipid-based formulation; the solution was placed in a capsule before dosing. Serial blood samples were obtained from a jugular vein of each dog before and at selected time points up to 48 h after dosing. Plasma concentrations of navitoclax and ABT-199 were determined by HPLC–tandem mass spectrometry. Platelets were measured using the AbbVie Cell-Dyn 3700 hematology analyzer. Platelet measurements were performed using an electrical impedance channel. Plasma concentration data were submitted to multiexponential curve fitting using WinNonlin. The area under the plasma concentration–time curve from 0 h to t h (time of the last measurable plasma concentration) after dosing (AUC_{0-t}) was calculated using the linear trapezoidal rule for the plasma concentration–time profiles. The residual area extrapolated to infinity, determined as the final measured plasma concentration (C_t) divided by the terminal elimination rate constant (β), was added to AUC_{0-t} to produce the total area under the curve ($AUC_{0-\infty}$). The dog studies were reviewed and approved by AbbVie's Lake County Institutional Animal Care and Use Committee. Animal studies were conducted in an Association for Assessment and Accreditation of Laboratory Animal Care–accredited program, and veterinary assistance was available to ensure appropriate animal care.

Reagents. ABT-199 (4-(4-{[2-(4-chlorophenyl)-4,4-dimethylcyclohex-1-en-1-yl]methyl}piperazin-1-yl)-*N*-({3-nitro-4-[(tetrahydro-2*H*-pyran-4-ylmethyl)amino]phenyl}sulfonyl)-2-(1*H*-pyrrolo[2,3-*b*]pyridin-5-yloxy)benzamide) and other small-molecule inhibitors of proteins in the BCL-2 family described were synthesized at AbbVie Inc. (North Chicago, IL). Rituximab was purchased from Genentech, Inc. (South San Francisco, CA). Bendamustine was purchased from Cephalon, Inc. (Frazer, PA). Phosal 50 PG was purchased from American Lecithin (Oxford, CT).

Clinical dosing of patients with cancer. The first-in-human trial of ABT-199 ("A Phase 1 Study Evaluating the Safety and Pharmacokinetics of ABT-199 in Subjects With Relapsed or Refractory Chronic Lymphocytic Leukemia and Non-Hodgkin's Lymphoma," ClinicalTrials.gov identifier NCT01328626) involves exposure to a single oral dose followed by safety and pharmacokinetic monitoring before subjects progress to an ongoing continuous-dosing phase. The study is ongoing and being conducted according to the Declaration of Helsinki and relevant International Conference on Harmonization Good Clinical Practice guidelines and with approval from the HRECs of the Peter MacCallum Cancer Centre and Melbourne Health. Only data for the first three doses given to the first three subjects (two females and one male) are included in this manuscript. All had poor prognosis CLL refractory to standard therapy and met all inclusion and exclusion criteria. All provided written informed consent before participating in this study.

47. Zhang, H., Nimmer, P., Rosenberg, S.H., Ng, S.C. & Joseph, M. Development of a high-throughput fluorescence polarization assay for Bcl-x(L). *Anal. Biochem.* **307**, 70–75 (2002).
48. Chen, J. *et al.* The Bcl-2/Bcl-X(L)/Bcl-w inhibitor, navitoclax, enhances the activity of chemotherapeutic agents *in vitro* and *in vivo*. *Mol. Cancer Ther.* **10**, 2340–2349 (2011).
49. Phillips, D.C., Garrison, S.P., Jeffers, J.R. & Zambetti, G.P. Assays to measure p53-dependent and -independent apoptosis. *Methods Mol. Biol.* **559**, 143–159 (2009).
50. Mason, K.D. *et al.* The BH3 mimetic compound, ABT-737, synergizes with a range of cytotoxic chemotherapy agents in chronic lymphocytic leukemia. *Leukemia* **23**, 2034–2041 (2009).

doi:10.1038/nm.3048